Novel Tm^{3+}-doped transparent fluorozirconate glass-ceramic containing nanocrystalline

Yangqiong Lai (赖杨琼)[1,2], Junjie Zhang (张军杰)[1], Chunlei Yu (于春雷)[1,2], and Lili Hu (胡丽丽)[1]

[1]*Shanghai Institute of Optics and Fine Mechanics, Chinese Academy of Sciences, Shanghai 201800*

[2]*Graduate School of the Chinese Academy of Sciences, Beijing 100049*

Received May 12, 2006

A new transparent Tm^{3+}-doped ZrF_4-based nanocrystallized glass with the composition of $55ZrF_4$-$20BaF_2$-$18.8YF_3$-$5AlF_5$-$1.2TmF_3$ (mol%) (ZBYA) has been prepared by a conventional melting quenching technique and the subsequent heat treatment processes. The glass characteristic temperatures, the apparent activation energy, and the Avrami parameter for crystallization are estimated on the basis of different scanning calorimetry (DSC). The sizes of grown nanocrystals in the glass matrix appear to be 30—36.5 nm and it is studied as a function of the nucleation temperature, also the peak intensity of the nanocrystalline is studied as a function of the nucleation temperature from the X-ray diffraction (XRD) measurement. The microhardness measurement shows that the Vickers microhardness (H_v) values of the heat-treated glass samples are larger than that of the based glass about 17.26%—42.04%.

OCIS codes: 160.4760, 160.5690, 160.2120, 160.2750.

The ZrF_4-based heavy-metal fluoride glasses containing rare earth (RE) ions have excellent optical properties that make them have potential application in fiber amplifier, upconversion lasers, and three-dimensional displays[1−3]. However, their mechanical properties are poor as comparing with those of other more-traditional window materials. In fact, their poor mechanical properties limit their usefulness in severe environment. In addition, the relatively poor stability of ZrF_4-based heavy-metal fluoride glasses with respect to well-known spontaneous crystallization has hindered their development and application[4,5].

Up to now, the glass ceramic has been extensively used to enhance the mechanical and thermal properties of silica glasses. Recently, this attempt has also been done with zirconium fluoride-based glass-ceramics to increase the mechanical resistance and optical properties. In this way, many glass ceramics have been obtained by nucleation and growth at various temperatures and times[6]. When the RE ion is only in the microcrystalline phase of the fluoride type, it would improve the emission and laser properties of the medium: elongate lifetimes of fluorescent states, reduce inhomogeneous line-width, and increase cross-section[3,7,8]. In 1996, Auzel *et al.* reported a new transparent Er^{3+}-doped fluoride glass-ceramic showing only nanocrystallized phase type which contained the RE ion, there is high potential as a new amplification medium[7]. However, this fluoride glass system has lower stability, and usually there are some crystallites whose sizes are larger than the wavelength, it causes the important light scattering which is useful for display purposes and prevents the use of the fluoride glass-ceramic. From Ref. [6], we know that it is very difficulty to obtain transparent glass-ceramic system by spinodal decomposition in multicomponent zirconium-fluoride-based glass, also there is little information about stable glass-ceramic containing bivalent metal. In this study, a novel Tm^{3+}-doped transparent glass-ceramic containing nanocrystalline has been successfully prepared and the transparent glass-ceramic has much higher H_v values than the based glass. In this material, the Tm^{3+} ion acts as nucleating agents[6]. In addition, we investigate the nanocrystalline phases appearing in the glassy matrix by X-ray diffraction (XRD), the activation energy for crystallization together with glass transformation and the crystallization temperatures are estimated on the basis of different scanning calorimetry (DSC).

Tm^{3+}-doped $55ZrF_4$-$5AlF_5$-$20YF_3$-$20BaF_2$ (mol%) glass was prepared by using conventional melt quenching technique. The anhydrous powders of ZrF_4, AlF_5, YF_3, BaF_2, and TmF_3 with more than 99.9% purity were used as starting materials. Batches of 50-g powders with NH_4HF_2 were mixed thoroughly and transferred to platinum crucibles, which was placed in an electrically heated furnace in air atmosphere. When stirred and refined at 1000 °C for 1 h, the glass was cast into a heated copper mold. After 30-min relaxation time, the glass samples were cooled to ambient temperature at a rate of 2 °C/min to ensure identical thermal history. After that, the heat treatments from 330 to 400 °C for 4 h were performed to precipitate crystals. The glass transition temperature (T_g) and onset crystallization temperature (T_x) were measured by a Perkin-Elmer differential scanning calorimeter. The DSC curves were measured with rates of 2,5,10, 15, 20 °C/min for the glass. The XRD measurements (Rigaku Inc.D\max-2550X, Japan) of the crushed powders of the as quenched and heat-treated samples at different temperatures were carried out with 2θ from 10° to 80°; The surface hardness of the glass samples was determined on the basis of Vickers hardness, the Vickers microhardness (H_v) measurements were performed with a Shimadzu microhardness tester and for each sample the values of H_v were determined on the basis of at least five indentation measurements on the flat surface of the specimen. All the measurements were carried out at room temperature.

Figure 1 shows the DSC traces for the as-melted glass and the heat-treated glass samples ($55ZrF_4$-$20BaF_2$-

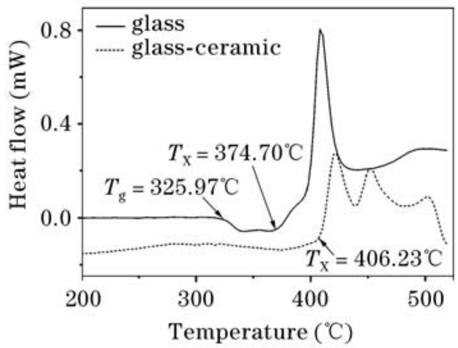

Fig. 1. DSC traces for ZBYA glass and glass-ceramic.

$18.8YF_3$-$5AlF_5$-$1.2TmF_3$ (mol%) (ZBYA)). The heat-treated glass sample was firstly heated at 345 °C for 4h and then at 380 °C for 20 min. The glass transformation temperature and the onset crystallization temperature for the as-melted glass are 325.97 and 374.70 °C, respectively. After heat treatment to form a glass-ceramic, the glass transition temperature becomes indistinct, and the onset crystallization temperature increases to 406.23 °C, this indicates that there are some crystallites formed in the glass matrix[9−11].

The part of DSC curves covering only the crystallization peak region is shown in the Fig. 2. The apparent activation energy for crystallization E_a was determined by plotting: $\ln(T_p^2/\alpha)$ versus $1/T_p$ (see Fig. 3), where α is the heating rate and T_p is the temperature

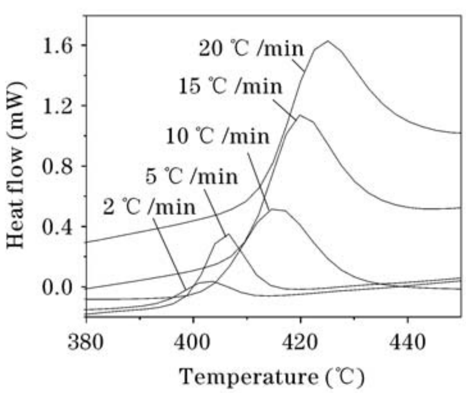

Fig. 2. Evolution of the position of crystallization peaks versus heating rate.

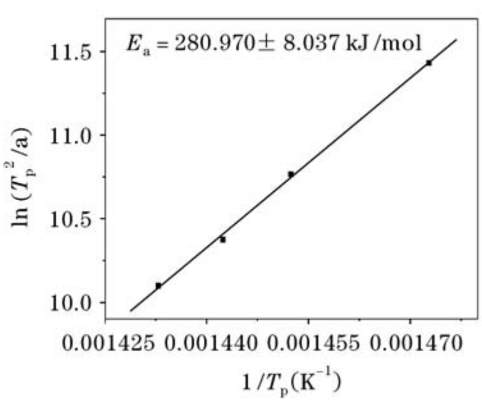

Fig. 3. Determination of the activation energy on the basis of DSC results.

of the maximum of the crystallization peak on DSC curve, according to the method described by Chen[12]. Also the Avrami parameter was determined by using the equation[13] $n = \frac{2.5RT_p^2}{\Delta T E_\alpha}$, where ΔT is used as a measure factor of the stability of a glass and its value is $T_x - T_g$, R is the universal gas constant. The estimated activation energy for crystallization is 280.97 kJ/mol and values of Avrami parameters for all the glasses at different nucleation temperatures are given in Table 1. A value of $n \approx 2$ indicates surface crystallization. Values of n ranging between 3 and 4 indicate bulk crystallization occurring in a three-dimensional (3D) growth pattern, with $n \approx 3$ indicating a constant number of nuclei, and $n \approx 4$ indicating time-dependent nucleation[10]. The values of n for the glasses nucleation at 330 and 335 °C are in agreement with the observed surface crystallization that occurs for those samples, and with n increasing from 1.93 to 3.75, the crystallization goes from surface controlled to bulk controlled by increasing the nucleation temperature.

Table 1. Parameters from Fit to the Avrami Equation

Nucleation Temperature (°C)	Avrami Parameter (n)
330	1.93
335	2.21
340	3.32
345	3.75
350	3.56

The powder XRD patterns for the glass and heat-treated crystallized samples are shown in Fig. 4. The peaks at around $2\theta = 22.5°$ and 28.2° found by a computer-assisted Boolean search of existing powder diffraction reference pattern are attributed to the crystallites of β-$BaZrF_6$[5]. Compared to the powder XRD pattern of glass sample, the appearance of some strong peaks of heat-treated glass samples indicates that there are some crystallites formed in the glass matrix. The effect of nucleation temperature on the peak intensity of β-$BaZrF_6$ is shown in the Fig. 5. From the peak intensity of β-$BaZrF_6$ around $2\theta = 22.5°$, we can conclude that the nuclei density increases with increasing nucleation temperature[5].

The results of the diameters of the crystalline particles are shown in the Fig. 6. The diameters of the crystalline

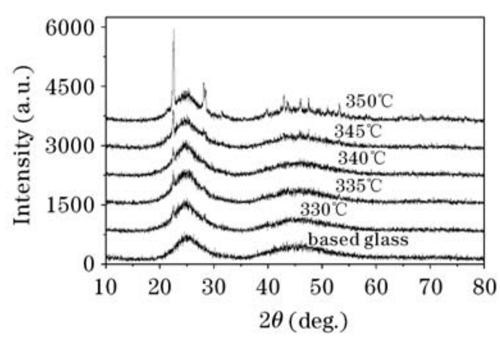

Fig. 4. Powder XRD pattern at room temperature for the based glass and heat-treated samples. The five heat-treated samples are treated at 330 °C, 335 °C, 340 °C, 345 °C, and 350 °C respectively for 4 h, and then at 380 °C for 20 min.

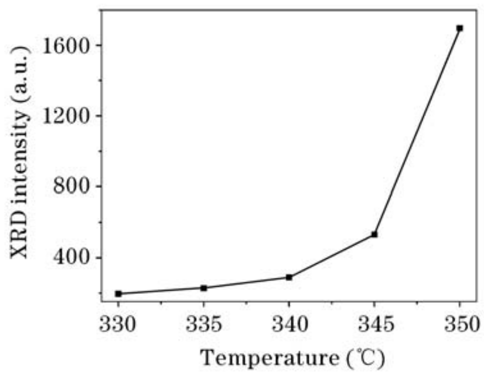

Fig. 5. XRD intensity of the peak of β-$BaZrF_6$ versus nucleation temperature.

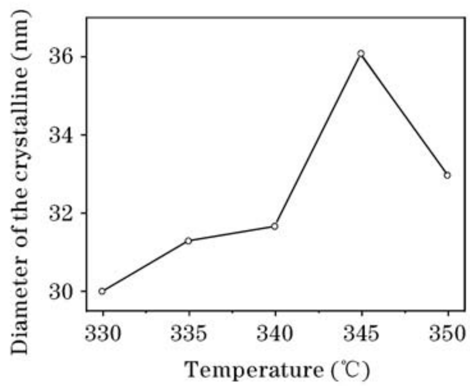

Fig. 6. Diameter of the crystalline particles versus nucleation temperature.

Table 2. Vickers Hardness Values of the Based Glass and Transparent Crystallized Glasses

	Based Glasses	Crystallized Glasses: 335 °C for 4 h and then 380°C for 20 min	Crystallized Glasses: 350 °C for 4 h and then 380 °C for 20 min
H_v (GPa)	2.26	2.65	3.21

particles were estimated by using Scherrer's equation: $D = K\lambda/\beta\cos\theta$, where D is the diameter of the crystalline particle, K the Scherrer constant, λ the X beam wavelength, β the full-width at half-maximum (FWHM) of a XRD peak, and θ the diffraction angle. The sizes of crystals increase with increasing nucleation temperature and reach a maximum near 345 °C. The Vickers microhardness (H_v) values of three samples are listed in Table 2. The transparent nanocrystallized glass has much higher H_v values than the base glass about 17.25%—42.03% and the H_v values in higher nucleation temperature are usually higher than those in lower temperature.

The optical transmission spectra of three samples are shown in Fig. 7. The optical transmission for the as-melted glass is nearly 90% between 360—630 nm, the optical transmission for the heat-treated glass samples 2 and 3 are all over 80% between 360—630 nm. It is found that the decrease in the transmission for the heat-treated glass samples is small. The prepared fluoride glass ceramics in this work are very transparent, the

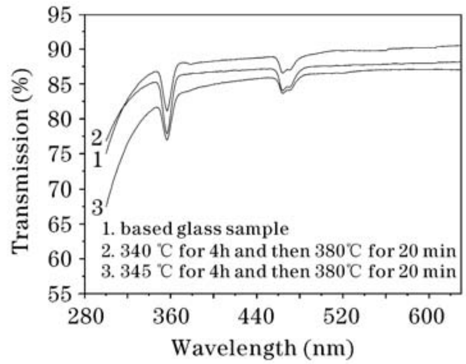

Fig. 7. Optical transmittance spectra for the based glass and heat-treated glass samples.

transparency can be clearly seen by the naked eyes.

The appearing of the transparent fluoride glass-ceramic gives us a mean of improving the mechanical properties, which can overcome the limitation on application imposed by the poor physical properties of fluoride glasses. One of the most outstanding experiment results is that we have successfully prepared the transparent Tm^{3+}-doped ZrF_4-based nanocrystallized glasses with the composition of $55ZrF_4$-$5AlF_5$-$18.8YF_3$-$20BaF_2$-$1.2TmF_3$ (mol%). The increase in the Vickers hardness values of heat-treated samples due to nanocrystallization has high resistance against deformation compared with the based glass. The diameters of the crystalline particles and the intensity of peak of nanocrystalline increase with increasing nucleation temperature.

This work was supported by the "Rising-Star" Project of Shanghai Municipal Science and Technology Commission (No. 04QMX1448), and the National Natural Science Foundation of China (No. 50572110). J. Zhang is the author to whom the correspondence should be addressed, his e-mail address is jjzhang@mail.siom.ac.cn.

References

1. M. Poulain, J. Non-Cryst. Solids **184,** 103 (1995).
2. J.-L. Adam, J. Fluorine Chem. **107,** 265 (2001).
3. W. A. Pisarski, J. Pisarska, T. Goryczka, G. Dominiak-Dzik, and W. Ryba-Romanowski, J. Alloys and Compounds **398,** 272 (2005).
4. K. E. Lipinska-Kalita, F. Auzel, and P. Santa-Cruz, J. Non-Cryst. Solids **204,** 188 (1996).
5. H. Ebendorff-Heidepriem, I. Szabó, and Z. E. Rasztovits, Opt. Mater. **14,** 127 (2000).
6. M. Mortier, A. Monteville, G. Patriarche, G. Maze, and F. Auzel, Opt. Mater. **16,** 255 (2001).
7. F. Auzel, K. E. Lipinska-Kalita, and P. Santa-Cruz, Opt. Mater. **5,** 75 (1996).
8. P. Santa-Cruz, D. Morin, J. Dexpert-Ghys, A. Sadoc, and F. Auzel, J. Non-Cryst. Solids **190,** 238 (1995).
9. J. M. Jewell, E. J. Friebele, and I. D. Aggarwal, J. Non-Cryst. Solids **188,** 285 (1995).
10. J. M. Jewell, E. J. Friebele, and I. D. Aggarwal, J. Am. Ceram. Soc. **79,** 2397 (1996).
11. J. M. Jewell, J. Jaganathan, and I. D. Aggarwal, J. Am. Ceram. Soc. **74,** 788 (1991).
12. H. S. Chen, J. Non-Cryst. Solids **27,** 257 (1978).
13. J. A. Augis and J. E. Bennett, J. Therm. Anal. **13,** 283 (1978).